

Date of publication xxxx 00, 0000, date of current version xxxx 00, 0000.

Digital Object Identifier 10.1109/ACCESS.2017.DOI

Biomechanical Ambulatory Assessment of 3D Knee Angle Using Novel Inertial Sensor-Based Technique

LAI KUAN THAM¹, NOOR AZUAN ABU OSMAN^{1,2}, MOUAZ AL KOUZBARY¹, AND KAMIAR AMINIAN³, (SENIOR MEMBER, IEEE)

¹Centre for Applied Biomechanics, Department of Biomedical Engineering, Faculty of Engineering, University of Malaya, Kuala Lumpur, Malaysia.

²BioApps Sdn. Bhd., University of Malaya Medical Centre, Kuala Lumpur, Malaysia.

³Laboratory of Movement Analysis and Measurement, École Polytechnique Fédérale de Lausanne, 1015 Lausanne, Switzerland.

Corresponding author: Noor Azuan Abu Osman (e-mail: azuan@um.edu.my).

This work was funded by BioApps Sdn. Bhd. and Platcom HIP-2 (AIM/PlaTCOM/HIP2/CCGF/2017/168).

ABSTRACT Three-dimensional (3D) knee angle measurement is one of the key measures in human gait analysis. Inertial sensor capable of measuring joint motion under unconstrained conditions is a practical tool for clinical evaluation and rehabilitation. An inertial measurement unit (IMU) consisting of accelerometer and gyroscope allows orientation measurement in 3D with an additional sensor (i.e., magnetometer). However, ferromagnetic interference negatively affects the performance of magnetometer and thus reduces measurement accuracy. In this study, a technique based on nonlinear autoregressive neural network with exogenous inputs (NARX) is presented to measure 3D segmental orientation during gait without the use of magnetometer. With IMUs attached to the thigh and shank, 3D knee angles in long-distance treadmill walking were computed and validated against an optical motion analysis system as the gold standard. Pseudo-integrator (PI) was also compared to the reference system for benchmarking. The learning capability of NARX was further assessed with the comparison of complementary filter (CF) to the reference system. The proposed NARX model was shown to outperform PI with biases between -3.5° and -0.2° , and root mean square errors between 4.5° and 2.5° . Results demonstrated the capability of NARX in providing accurate estimates of 3D knee joint angle while avoiding interference as encountered in systems incorporating magnetometer, suggesting that NARX is feasible to computing long-term ambulatory measurements of body segment orientation and 3D joint angles.

INDEX TERMS 3D knee angle, gait analysis, NARX network, pseudo-integration, segmental orientation.

I. INTRODUCTION

MEASUREMENT of three-dimensional (3D) knee angle is important in clinical and biomechanical applications for providing objective feedback, assisting diagnoses, evaluating the outcome of interventions, or orienting the rehabilitation of movement impairments [1]–[4]. In addition, knee angle is also a prime measure for control systems related to human exoskeleton and robotic prostheses [5]. Generally, human movement is qualitatively assessed by visual observation in clinical environment [3], [6]. Objective assessment based on stereophotogrammetry involving motion capture cameras enables accurate measurement of 3D joint angles in laboratory settings. Such system, however, requires high setup cost, sophisticated equipment, and specialized personnel and space. Moreover, the number of gait cycle is limited

by the confined space, thus restricting its widespread use in clinical assessments [7]–[10].

In recent years, the emerging technology of micro-electro-mechanical systems (MEMS) has become the main contributor to the development of wearable sensors. Miniature inertial sensors are comfortable to wear and easy to setup, providing an alternative to gait assessment [11]. Ambulatory systems consisting of wearable sensors have been applied in many studies to measure the kinematics and kinetics of normal and pathological gait [2], [10], [12].

In terms of lower limb kinematics, joint angles are commonly estimated using systems based on accelerometer, gyroscope, and magnetometer. Estimation of orientation using body-fixed gyroscopes is the simplest among all [8], [13], [14]. Time integration of angular velocity is applied to

calculate the orientation of an inertial sensor. Nevertheless, this method results in accumulated drift as the signals are integrated with superimposed noise over time [13], [15].

To remedy the problem of offset drift, approaches were proposed to reset a system using the periodical properties of gait. Morris first introduced the technique to equalize accelerometer data at the beginning and the end of each gait cycle [16]. Tong *et al.* identified the mid stance phase to reset angular velocity signals at each gait cycle [13]. Likewise, Williamson and Andrews and Liu *et al.* detected the mid stance phase using accelerometers and reset the integration of angular velocity by estimating segment inclination during this phase [14], [17]. Mayagoitia *et al.* utilized two accelerometers mounted perpendicular to each other on a body segment to estimate the reference angles during static period. The reference angles were then used to remove integration offset of angular velocity [8]. Takeda *et al.* estimated gravitational acceleration from cyclic accelerometer data to compute segment orientation during gait [7]. Drift removal using these approaches is only applicable to cyclic movements such as walking and running [10], [15].

Another alternative that prevents drift error is to avoid integration of angular velocity signals in orientation measurement. Using only accelerometers, acceleration signals from inertial sensors fixed on two adjacent segments were compared at the center of rotation. Willemsen *et al.* implemented the technique to estimate 2D joint angle using pairs of uniaxial accelerometers attached to the lower limbs [18]. Dejnabadi *et al.* developed a method which fused acceleration and angular velocity obtained from sensors placed on two neighboring segments. The method estimated acceleration of virtual sensors located at the center of rotation with respect to the physical sensors. 2D joint angle was then calculated by comparing acceleration of the two virtual sensors rotated to the same orientation at joint center [19], [20]. Takeda *et al.* calculated translational acceleration using angular velocity signals. Translational acceleration was then removed from acceleration data, producing gravitational acceleration that represents body segment inclination [21]. Liu *et al.* computed orientation by comparing data of two accelerometers attached to the same segment. Rotational acceleration was compared in this method while gravitational and translational acceleration, skin motion artifact, and other noise were considered equivalent on both sensor units [2]. Djuric *et al.* proposed a similar method to measure joint angles by comparing the difference in acceleration obtained from sensors mounted on rigid rods [22]. A drawback to this alternative is the decrease in accuracy of inclination estimation for movements involving high acceleration as the dynamic acceleration is indistinguishable from gravitational acceleration [23], [24].

Favre *et al.* developed a method fusing acceleration and angular velocity with a quaternion-based algorithm. Output drift was corrected by estimating inclination of the accelerometers during static phase [25]. The method has successfully captured 3D knee angles in a latter study. However, the technique was only accurate for short measurement time

since the transverse plane was not corrected in the algorithms [1]. Similar technique was implemented in Tadano *et al.*, correction for integration drift was performed using optical tracking system as the reference data. Performance of the method was affected by the resolution of images and the accuracy of optical cameras in tracking the reference markers [15].

In order to improve the accuracy of orientation estimate, the Kalman filter and the complementary filter are widely used in inertial sensor-based data fusion. The Kalman filter is a robust approach to integrate inertial data that provides good estimation accuracy. Inclination estimated from accelerometer was used to constantly correct offset error produced by the integration of angular velocity. There was, however, a heading error which restricted the approach to short-term measurements [26]. In addition, the efficiency of Kalman filter in angle estimation was found to be substantially reduced with fast movements [27], [28].

Gravity is generally adopted as the principal reference axis in all the above-mentioned alternatives, thus restricting measurement of segment orientation to only 2D. 3D orientation calculation is possible with a second reference axis such as the direction of foot progression introduced in Veltink *et al.* [29]. The method most commonly employed is the use of magnetic field from magnetometer as an additional reference axis [30]–[32]. Roetenberg *et al.* proposed a complementary Kalman filter incorporating signals from accelerometers, gyroscopes, and magnetometers. The model worked by assessing offset errors obtained from the integration of angular velocity and the estimation of inclination and magnetic field vector. These sources of information were weighed by the proposed filter to constantly recalibrate the inertial sensors for improved estimation of segment orientation [30], [31]. In O'Donovan *et al.*, gravity and magnetic field were used as the reference vectors to measure orientation during quasi-static movement. The static phase was also used to remove integration drift for orientation estimate during dynamic phase [32]. Šlajpah *et al.* performed long-term measurement of segment orientation using an extended Kalman filter to combine data from gyroscopes, accelerometers, and magnetometers. Orientation of each lower limb segment was estimated with a series of kinematic chain interconnecting the adjacent segments. The method produced larger error in segment involving higher acceleration which also decreased the accuracy of orientation estimates for the subsequent segments due to the chain relationship [12]. Meanwhile, Kalman filter that calculates orientation in greater accuracy requires estimation models with complicated state and measurement vectors and abundant recursive formulas, making the approach computationally demanding [33]. Furthermore, ferromagnetic interference remains an inevitable issue that reduces the efficiency of magnetometer and subsequently affects measurement accuracy [34].

A complementary filter (CF) generally consists of a low-pass filter and a high-pass filter to pass multi-sensory inertial signals, and in combination produces the final output [35].

Tian *et al.* and Fourati obtained better estimation of orientation by fusing the low frequency signals from the accelerometer and the high frequency signals from the gyroscope [33], [36]. The CF is well-known by its simplicity which enables effective measurement with lower computational cost. Accurate orientation estimates can be obtained using a complementary filter when the accelerometers function as inclinometers. However, estimation of acceleration-based orientation will be affected by linear acceleration for high acceleration motion. Furthermore, the accelerometer becomes incompetent in detecting orientation around axis parallel to the gravity and requires a third sensor (e.g., magnetometer) for 3D analysis.

Human ambulation dynamic was found to exhibit chaotic features in nature, its complexity is frequently investigated through nonlinear data processing methods [37]–[39]. As a common technique to predict nonlinear dynamic behavior, the general regression neural network (GRNN) has been applied by Findlow *et al.* to estimate 2D lower limb joint angles with reduced number of inertial sensors. Training of GRNN was conducted using kinematics data obtained from motion capture system, and joint angles on the sagittal plane were estimated using acceleration and angular velocity of the inertial sensors attached on the foot and shank. Intra-subject predictions produced high accuracy, while the inter-subject predictions showed lower correlations and larger variations between measured and estimated angles. A sufficiently large set of training data mapping more movement patterns was suggested to reduce the variability of inter-subject predictions using this approach. The suggestion, however, might be unachievable within a short time [40]. Moreover, a larger training sample for the GRNN will increase the network size and therefore the computational burdens [41]. One of the robust and commonly used techniques in prediction of complex nonlinear time series is a nonlinear autoregressive network model with exogenous inputs called the NARX [42], [43]. In Menezes *et al.*, it was shown that NARX outperform the topologies of other neural networks in chaotic time series estimation, providing further confirmation of the feasibility for the network model to be used in joint angle estimation [42].

Approaches presented in the literature demonstrated advancement of body segment orientation and joint angle estimate, from a general 2D to a comprehensive 3D measure. The common limitations of 3D orientation estimates include reduced accuracy in long-term measurements as the sensing axis of the transverse plane, which relies primarily on the magnetometer, is easily distorted by magnetic disturbance. Next, the efficiency of drift removal using system reset techniques that involved gait event detections is significantly affected in high-speed movements and pathological gait [34].

The objective of this study was therefore to provide long-term measurement of 3D joint angle while avoiding drawbacks from the above-mentioned issues. Firstly, as a mainstream method, lower limb segment angle was estimated in sagittal plane based on acceleration and angular velocity

measured by the inertial sensors using the CF. Secondly, a NARX model was developed to estimate segmental orientation where the outputs of CF were used as the target in training of the artificial neural network. This method is capable of computing 3D segmental orientation without the requirement of additional sensor (i.e., magnetometer) and the necessity of event detections for signals resetting. Thirdly, a method based on pseudo-integration which requires only gyroscopes was also replicated as benchmark to investigate the feasibility of the proposed NARX in estimating segmental orientation. The latter two methods were presented with the objective to provide long-term measurement of 3D joint angle while avoiding drawbacks from the above-mentioned literature. Accuracy of the presented methods was assessed by comparing knee joint angle to the reference measurement system at different walking speeds.

II. METHOD

A. SENSOR SYSTEM AND CALIBRATION OF COORDINATE SYSTEMS

A system comprised of four 6D inertial measurement units (IMUs) (Physilog[®], Gait Up, Lausanne, Switzerland) were used in this study. Each IMU (50mm × 40mm × 16mm, 36g) was made up of a 3D gyroscope (range: ±900°/s), a 3D accelerometer (range: ±11g), a radio transmitter, a microcontroller, a memory unit, and a battery. Signals of all synchronized sensor units were sampled on 16 bits at 500 Hz, low-pass filtered at 100 Hz, and recorded on the micro-SD card.

As shown in Fig. 1, raw signals of the thigh and shank sensors were represented in their respective sensors' technical frames (TFs), $u_T v_T w_T$ and $u_S v_S w_S$. In order to obtain data independent of sensor placements on the body, functional calibration procedures involving predefined posture and movements were carried out to align TFs of the sensors to the body anatomical frames (BAFs). First, the subject was asked to retain an upright standing posture to align the vertical axis, w_T to z_T and w_S to z_S , based on the gravity vector measured using accelerometer. Next, alignment of the lateral axis required the subject to perform movement that yield maximum angular velocity in a specific anatomical axis. For the thigh sensor, pitch angular velocity was optimized by performing hip abduction-adduction to align u_T to x_T . For the shank sensor, v_S was aligned to y_S by performing passive knee flexion-extension while the subjects sat upright with both feet dangling. Transformation of the TFs to the BAFs resulted in rotation matrices \mathbf{R}'_a and \mathbf{R}'_b for the thigh and shank respectively. Data measured by each IMU will be represented in its respective BAF and thus a global reference frame (GF) was required for knee angle calculation using the joint coordinate system (JCS) defined in Grood and Suntay [44].

The second phase of calibration involved transformation of the BAF to a GF, XYZ . Reflective markers were attached to the subject on sixteen anatomical landmarks following the Plug-in-Gait Marker Placement [45]. An optical motion anal-

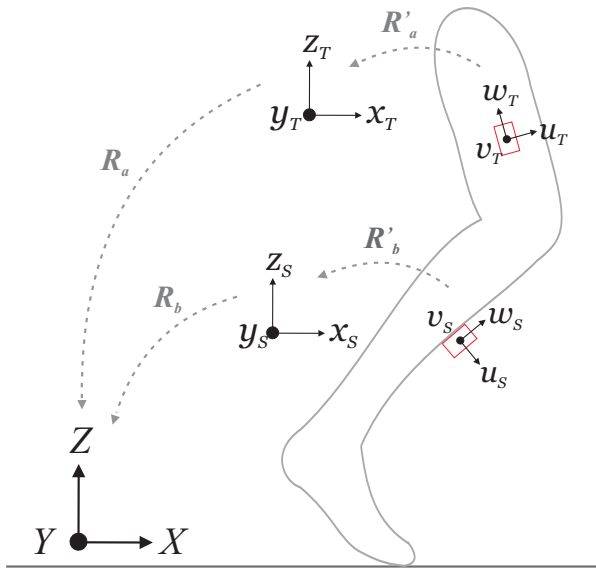


FIGURE 1. Definition of sensors' technical frames (TFs), body anatomical frames (BAFs), and global frame (GF). TFs of the thigh and shank sensors were represented in $u_T v_T w_T$ and $u_S v_S w_S$. Anatomical axes $x_T y_T z_T$ and $x_S y_S z_S$ represented the thigh and shank BAFs. GF was defined as the XYZ coordinate system.

ysis system Vicon Nexus 1.6 (Oxford Metrics, Oxford, UK) was used to capture calibration posture (i.e., upright standing) of the lower limbs. Using the trajectories of reflective markers tracked by the optical system, a wire frame model of the lower limb segments was produced. Rotation matrices \mathbf{R}_a and \mathbf{R}_b relating body segmental coordinate systems and global coordinate system could then be established. Finally, TFs of the thigh and shank sensors can be represented in the XYZ system using the rotation matrices \mathbf{R}_A and \mathbf{R}_B :

$$\mathbf{R}_A = \mathbf{R}'_a \mathbf{R}_a \text{ and } \mathbf{R}_B = \mathbf{R}'_b \mathbf{R}_b \quad (1)$$

B. ORIENTATION CALCULATION

In this study, body segmental orientation was estimated through three methods: the complementary filter as the de facto approach, while the feasibility of the NARX neural network and pseudo-integrator were also explored. All input signals for orientation estimates were aligned to the global reference frame.

1) Complementary Filter (CF)

The CF is known to be a robust and simple approach in multi-source data integration. The IMU consists of an accelerometer that gives inclination as angular position (p) during static conditions through a double integration of acceleration and a gyroscope that measured angular velocity (ν). Orientation estimate using the CF is based on p and ν , where the variables are related through $\nu = \dot{p}$ [33], [46].

The Laplace transform of angular position $P(S)$ admitted stable decomposition can be represented as:

$$P(S) = T_1(S)P(S) + T_2(S)P(S) \quad (2)$$

where $T_1(S) = k/(S+k)$, $T_2(S) = S/(S+k)$, and $T_1(S) + T_2(S) = 1$. $T_1(S)$ and $T_2(S)$ function as a lowpass and a highpass filter respectively. k is the filters' cutoff frequency.

Applying the relationship between $p(t)$ and $\nu(t)$, $P(S)$ can then be rewritten as:

$$P(S) = F_P(S)P(S) + F_N(S)N(S) \quad (3)$$

where $F_P(S) = T_1(S) = k/(S+k)$ and $F_N(S) = 1/(S+k)$ and $N(S) = SP(S)$.

Accelerometer ($P(S)$) which provides accurate measures at low frequency was filtered by the low-pass filter. On the other hand, gyroscope ($N(S)$) which suffers from low frequency errors was passed by a high-pass filter. Note that CF described in this study estimated two out of three orientation angles due to accelerometer indifference for rotation around any axes parallel to the axis representing gravitational field direction.

2) NARX Neural Network

NARX is a popular recurrent dynamic neural network which demonstrates outstanding performance in nonlinear time series predictions. It consists of memory units that store information in the input and hidden layers. The NARX model utilize the embedded memory as jump ahead connections for better learning capability and generalization performance [42], [47].

The main feature of the proposed NARX model is to produce orientation estimates through integration of angular velocity, low-frequency noise filtering, and elimination of gyroscopic drift, which can be described in equation (4):

$$P(S) = N(S) \cdot \frac{S}{S + \omega_c} \cdot \frac{1}{S} \quad (4)$$

where $P(S)$ and $N(S)$ are the output (i.e., position) and the input (i.e., angular velocity) respectively. ω_c is the low-frequency threshold based on operation bandwidth of the gyroscope. The intuition of equation (4) represented in discrete time domain can be applied to determine the number of input and output delay delays required in the NARX network structure.

Equation (4) can be represented in continuous time as follows:

$$\ddot{p} + \omega_c \dot{p} = \dot{\nu} \quad (5)$$

Using the Euler method of discretization with T_s as sample time, equation (5) can be represented in discrete form as shown in equation (6):

$$p_k = T_s \cdot \nu_k - T_s \cdot \nu_{k-1} + (2 + T_s \cdot \omega_c) \cdot p_{k-1} - p_{k-2} \quad (6)$$

Based on equation (6), the following signals are used as the NARX network inputs to anticipate body segment orientation: ν_k , ν_{k-1} , p_{k-1} , and p_{k-2} .

As illustrated in Fig. 2, training of the proposed NARX model started with the identification of input and output parameters. From the subjects' database containing segmental angular speed and position collected in gait trials, only gyroscope data in the sagittal plane was used as the input for NARX. Segmental orientation of the sagittal plane computed by the CF as described in Section II-B1 was selected as the desired output for the network. Next, the proposed NARX was trained using data of a 10 seconds training window (5000 samples) of a randomly selected subject walking at self-selected speed. Training of the NARX network was then progressed using the Levenberg-Marquardt backpropagation algorithm [48], [49]. Finally, the trained network is tested to ensure threshold error was achieved for optimal performance. The NARX is considered trained if the model can generalize CF performance in one plane (i.e., sagittal plane) to estimate orientation angles for all three planes.

An Optimized neural network requires minimization of layer and neuron number redundancy [50]. To have the least number of neurons, amplitude spectrum of the pre-processed gyroscope signals was analyzed. As shown in Fig. 3, gyroscopic signal captured by the shank IMU comprised of three major frequency components (i.e., 98 % of the signal power). This indicates that the signal must be disassembled to its main components by the proposed NARX model to process gait information whilst eliminating noise components. Thus, three neurons at the hidden layer are the minimum for the network to disassemble input signals.

Fig. 4 illustrates the proposed neural network structure to predict body orientation based on angular velocity. The network comprised of an input layer, a hidden layer with three neurons, and an output layer. Input parameters to the NARX model consisted of the normalized gyroscope signal (ν_k and ν_{k-1}) and the recurrent output of angular position (p_{k-1} and p_{k-2}). Distribution of synaptic weight between the processing neurons were determined with a particular threshold error in the training process. Activation function, $\sum(\cdot)$ and $f(\sum(\cdot))$, for the hidden and output layer are given in equation (7) and (8) respectively.

$$\sum(\cdot) = x_i \cdot w_{ij} + b_j \quad \forall \begin{cases} i \text{ inputs} \\ j \text{ number of neural} \end{cases} \quad (7)$$

$$f(\sum(\cdot)) = \begin{cases} \frac{1 - e^{-2\sum(\cdot)}}{1 + e^{-2\sum(\cdot)}} & \text{at hidden layer} \\ \sum(\cdot) & \text{at output layer} \end{cases} \quad (8)$$

where x is the incoming data, w is the connection weight, and b represents the bias term.

The output parameter was denormalized at the last stage producing segmental orientation.

3) Pseudo-integrator (PI)

Holgate *et al.* proposed the method of pseudo-integration that used gyroscopes to measure tibia angle in a tibia-based controller for powered ankle-foot prosthesis [51]. PI was

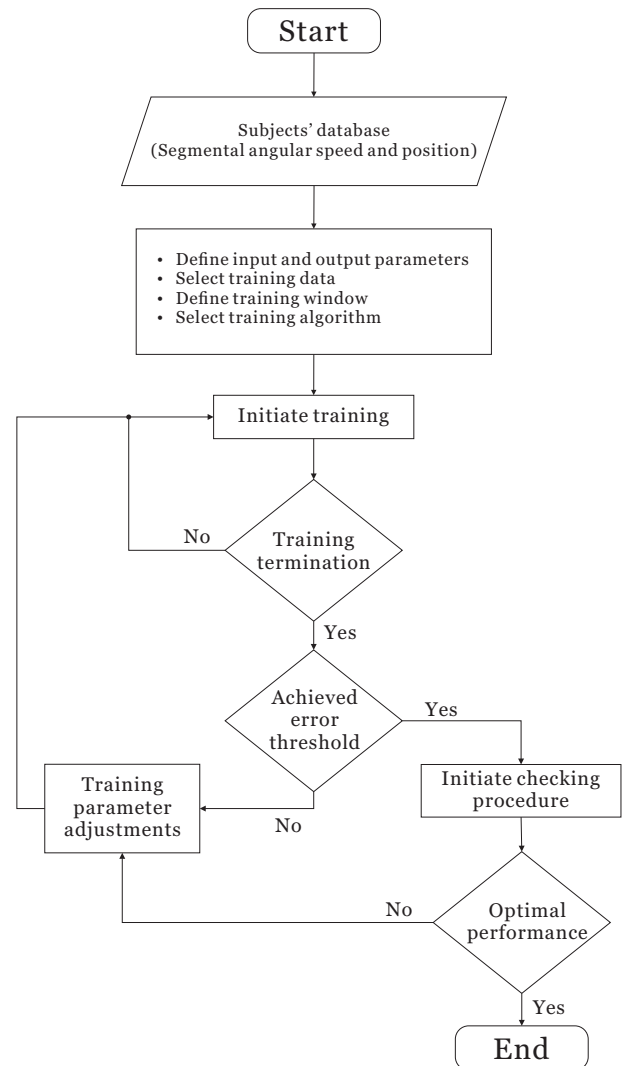


FIGURE 2. Schematic flow chart for the NARX neural network training. The NARX was trained with gyroscope data of the sagittal plane as input and segmental orientation of the sagittal plane computed by the CF as target output.

replicated in this study as a benchmark method for orientation estimates using only gyroscope data (i.e., angular velocity). The main idea of the method was based on the transfer function (equation 9) which has an asymptote close to -90 dB/decade:

$$\frac{\tau^2 S}{(\tau S + 1)^2} \quad (9)$$

where $\tau = 1/\omega_n$ and ω_n is the breakpoint frequency. The breakpoint frequency was calculated as the gait frequency in this study.

The major issue of angle measurement using gyroscopes is the accumulated drift as a consequence of integrating angular velocity with the underlying noise. In terms of transfer function, integration drift is due to the marginally-stable nature of an integrator which has a pole on the origin. In contrast, PI

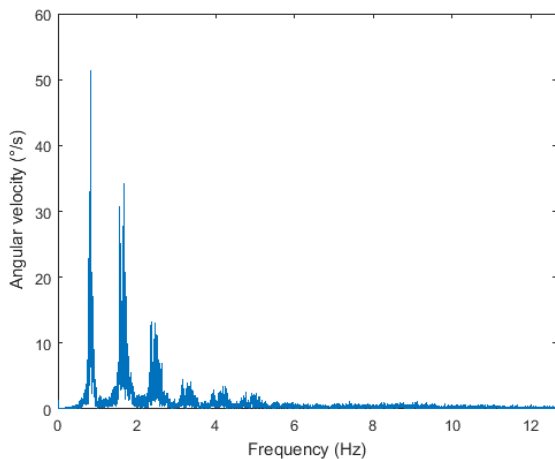


FIGURE 3. Single-sided amplitude spectrum of shank gyroscope during gait. Three major frequency components were observed.

TABLE 1. Demographic characteristics of the subjects

Subject	Gender	Age (years)	Height (m)	Mass (kg)
S1	F	28	1.62	48
S2	M	33	1.84	84
S3	F	22	1.59	49
S4	M	24	1.79	75
S5	F	27	1.59	55

has two real stable poles, thus producing a stable system with drift removal property.

The PI transfer function can be analyzed as a high-pass filter and an active low-pass filter with amplifying gain based on ω_n value, as shown in Fig. 5. The combination of the filters is a band-pass filter which pass gyroscopic signals around gait frequency.

The initial conditions for NARX network and PI buffers were regarded as zeros in order to reduce memory usage and enhance estimation capability for real-time calculation.

C. EXPERIMENTAL VALIDATION

The presented algorithms were validated with indoor experiments of gait assessment. Five healthy volunteers (2 males and 3 females, 26.8 ± 4.2 years old, 1.7 ± 0.1 m, 62.2 ± 16.3 kg) with no past and present history of musculoskeletal, neuromuscular or cardiovascular disorders were enrolled in this study. All volunteers gave informed consent before enrollment and their demographic characteristics are shown in Table 1. None of the subjects possessed injuries or illness at the day of experiment.

The thigh (lateral side of the quadriceps) and shank (shaft of the tibia) that produce minimal motion artifacts were fixed with one sensor unit respectively, on both sides, using elastic Velcro straps. Reflective markers were attached on sixteen anatomical landmarks following the Plug-in-Gait Marker Placement [45]. An optical motion analysis system Vicon Nexus 1.6 (Oxford Metrics, Oxford, UK) was used to capture

movements of the reflective markers during the trials as the reference measure of this study.

Volunteers were first asked to perform functional calibration as described in section II-A, followed by treadmill walking. Each volunteer spent minimum 15 minutes walking on the treadmill at the speed that they felt comfortable, to adapt and be familiar with the treadmill. The indicated speed was then selected as the normal gait speed, while the fast and slow speeds were established as $\pm 30\%$ of the normal gait speed. Measurements involved one 5 minutes trial at the normal, fast, and slow gait speeds on the treadmill. Trials were performed in random order; the participants were given 5 to 10 minutes for recovery between each trial. All volunteers gave informed consent prior to trial participation. The experiment was approved by the local medical research and ethics committee.

D. DATA ANALYSIS

3D lower limb segment orientation for the sensor system was estimated by NARX and PI, and compared to orientation measured by the optical system (reference). CF which computed orientation in 2 degrees of freedom (2-DoF) was compared to the reference system as a secondary measure to evaluate the performance of NARX. Thigh and shank orientation transformed to the GF were then used to calculate knee joint angles following the JCS definition recommended by the ISB [1], [44]. CF computed knee angles in 2D (i.e., sagittal and frontal plane), and computation of 3D knee angle was performed using NARX network and PI. Estimation errors defined as the difference between knee angles estimated with the reference system and the described methods were computed and represented as the mean and standard deviation (SD), indicating bias and precision. The bias and precision of each algorithm in the sagittal plane can be calculated using equation (10) and equation (11); similar formulas were used in the frontal and transverse plane.

$$Bias_{sagittal} = mean\left(\sum_n \theta_{m|ref} - \theta_{m|x}\right) \quad (10)$$

$$Precision_{sagittal} = SD\left(\sum_n \theta_{m|ref} - \theta_{m|x}\right) \quad (11)$$

where θ is the knee angle, n is the total number of subjects, m is the number of samples, ref is the reference system, and x indicates the method.

Agreements between the proposed methods and the reference system were quantified by the root mean square errors (RMSEs) and Pearson's correlation coefficients (r). The limits of agreement between knee angle measurements were also investigated through the Bland-Altman plots [52].

All analysis and statistical evaluations were performed in MATLAB (version 2019a, The Mathworks Inc., Natick, MA, USA) and SPSS Statistics (version 22, IBM SPSS Inc., Chicago, IL, USA).

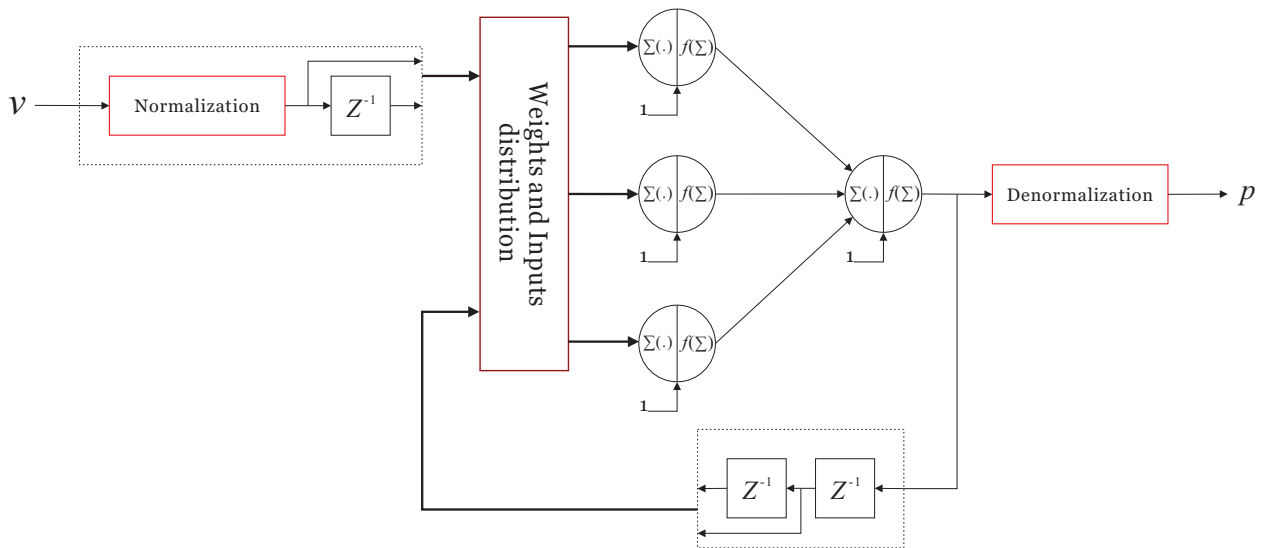


FIGURE 4. NARX network structure to estimate body segment orientation based on gyroscopic signal. The NARX model composed of an input layer, a hidden layer with three neurons, and an output layer. Normalized gyroscope signals (ν) and recurrent output were received at the input layer to produce segmental orientation (p) as the output after denormalization.

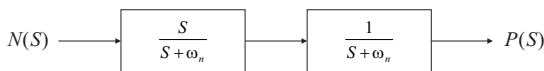


FIGURE 5. Model of pseudo-integrator to estimate body segment orientation. Angular velocity (N) was processed using the S-domain transfer function that combined a high-pass and an active low-pass filter with amplifying gain based on breakpoint frequency (ω_n) to output orientation (P).

III. RESULTS

Comparison of knee angle measured by the presented methods and the reference system consisted a total of 3794 gait cycles, excluding time samples with marker occlusions. The sample size for slow (2.6 ± 0.2 km/h), normal (3.3 ± 0.2 km/h), and fast (4.3 ± 0.3 km/h) walking speed was 1109, 1272, and 1413 cycles, respectively. Fig. 6 shows a typical plot of 3D knee angle computed by the presented methods along with the reference system in a random 10 seconds window during the first and fifth minute of normal speed walking. As shown in Fig. 6, all presented methods exhibited minimal drift effect across the trial time, demonstrating the feasibility and reliability in long-distance measurement.

Table 2 demonstrates the knee angle errors of the sagittal plane, which correspond to knee flexion-extension. The NARX model produced bias \pm precision of $-0.4 \pm 2.5^\circ$, $-0.3 \pm 2.2^\circ$, and $-0.3 \pm 2.5^\circ$ and RMSE of $3.2 \pm 0.2^\circ$, $2.7 \pm 0.2^\circ$, and $3.6 \pm 0.3^\circ$ for slow, normal, and fast speed, respectively, which was the lowest of all presented methods. However, agreements to the reference system were slightly better in CF, with the r values of 0.99 for all level walking speeds.

TABLE 2. Error ($^\circ$), RMSE ($^\circ$) and correlation coefficient (r) between proposed methods and reference system in the sagittal plane during slow, normal, and fast speed level walking

		Error		RMSE		r	
		mean	SD	mean	SD	mean	SD
Slow	CF	-2.8	3.2	3.8	0.3	0.99	0.00
	NARX	-0.4	2.5	3.2	0.2	0.98	0.00
	PI	-3.3	3.9	5.1	0.3	0.97	0.00
Normal	CF	-2.6	2.7	3.4	0.2	0.99	0.00
	NARX	-0.3	2.2	2.7	0.2	0.99	0.00
	PI	-2.8	3.4	4.4	0.2	0.98	0.00
Fast	CF	-4.6	3.8	5.1	0.5	0.99	0.00
	NARX	-0.3	2.5	3.6	0.3	0.98	0.00
	PI	-4.4	3.5	5.6	0.3	0.98	0.00

For frontal plane (i.e. knee abduction-adduction) comparisons summarized in Table 3, NARX demonstrated the best performance in knee angle estimates with the bias \pm precision of $-1.0 \pm 3.3^\circ$, $-0.9 \pm 3.8^\circ$, and $-0.2 \pm 3.4^\circ$ for slow, normal, and fast walking, respectively. Similarly, NARX reported the lowest RMSE of $2.5 \pm 0.6^\circ$, $2.7 \pm 0.3^\circ$, and $2.9 \pm 0.3^\circ$ in slow, normal, and fast walking speeds. Correlation assessment also showed the highest r values of 0.96, 0.95, and 0.95 for slow, normal, and fast walking in NARX.

Table 4 shows the assessment of knee angle measurement in the transverse plane, corresponding to knee internal-external rotation, for NARX and PI. In general, NARX demonstrated the lowest bias and RMSE and the highest correlation to the reference system. The bias \pm precision values obtained were $-3.2 \pm 2.9^\circ$, $-3.5 \pm 2.8^\circ$, and $-1.8 \pm 2.8^\circ$ whereas the RMSE values were $4.3 \pm 0.1^\circ$, $4.5 \pm 0.6^\circ$, and

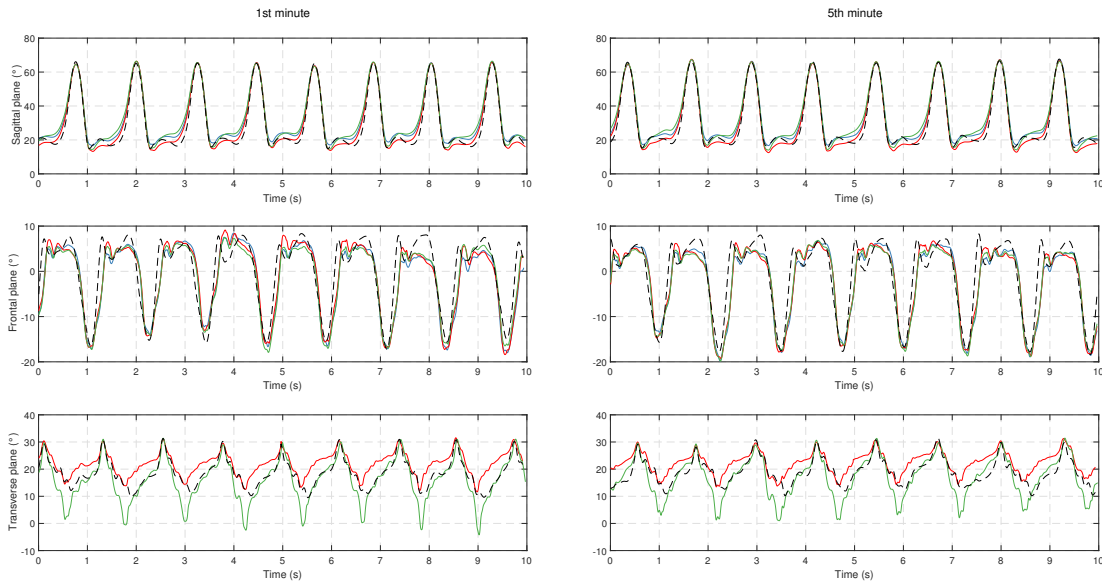


FIGURE 6. Exemplar of 3D knee angle computed by the proposed NARX neural network (red line), pseudo-integrator (green line), complementary filter (blue line), and reference system (dashed line) in a random 10 seconds window during the 1st and 5th minute of normal speed walking.

TABLE 3. Error ($^{\circ}$), RMSE ($^{\circ}$) and correlation coefficient (r) between proposed methods and reference system in the frontal plane during slow, normal, and fast speed level walking

		Error		RMSE		r	
		mean	SD	mean	SD	mean	SD
Slow	CF	-2.0	3.3	2.7	0.6	0.96	0.02
	NARX	-1.0	3.3	2.5	0.6	0.96	0.02
	PI	-1.7	3.4	2.7	0.5	0.96	0.02
Normal	CF	-1.6	3.9	2.8	0.4	0.95	0.02
	NARX	-0.9	3.8	2.7	0.3	0.95	0.02
	PI	-1.5	3.7	2.8	0.3	0.95	0.01
Fast	CF	-1.2	3.5	3.0	0.3	0.94	0.01
	NARX	-0.2	3.4	2.9	0.3	0.95	0.01
	PI	-1.1	3.6	3.3	0.3	0.92	0.01

TABLE 4. Error ($^{\circ}$), RMSE ($^{\circ}$) and correlation coefficient (r) between proposed methods and reference system in the transverse plane during slow, normal, and fast speed level walking

		Error		RMSE		r	
		mean	SD	mean	SD	mean	SD
Slow	NARX	-3.2	2.9	4.3	0.1	0.84	0.07
	PI	4.1	3.8	5.4	1.3	0.80	0.05
Normal	NARX	-3.5	2.8	4.5	0.6	0.83	0.03
	PI	2.4	4.4	5.0	0.1	0.82	0.07
Fast	NARX	-1.8	2.8	3.4	0.4	0.84	0.05
	PI	4.8	5.8	7.0	1.9	0.75	0.40

$3.4 \pm 0.4^{\circ}$ for slow, normal, and fast speed, respectively. The r values were 0.84, 0.83, and 0.84 for slow, normal, and fast level walking. Note that CF is not available for measuring transverse plane rotation (see Fig. 6 and Table 4) as the 6D IMUs were used in this study.

NARX reported the best performance in terms of accuracy and precision for all knee angle estimates categorized into anatomical planes. Thus, further analysis on the limits of agreement involved only the proposed NARX model.

Fig. 7 illustrates the Bland-Altman plots of the difference between 3D knee angles computed with NARX and the reference system in different walking speeds (2.6 to 4.3 km/h). The biases are within 95% limits of agreement (i.e., ± 1.96 SD) except for some minor outliers in fast walking of the sagittal plane, slow and fast walking of the frontal plane, and slow walking of the transverse plane.

IV. DISCUSSION

A wearable system of inertial sensors with new algorithm for the assessment of 3D knee angles during long-distance level walking was presented in this paper. Knee orientation computation using inertial signals was based on (1) a NARX neural network and (2) a pseudo-integrator (PI). The NARX model trained with sagittal plane angles calculated by a complementary filter (CF) required only angular velocity as the input in segmental orientation estimates. PI, which also used gyroscope signals as the only input, was replicated in this study for benchmarking the performance of NARX. Performance assessment of the proposed methods was presented as comparisons with a reference optical motion analysis system. Additionally, to justify the capability of NARX in replicating the behavior of CF using only gyroscope signals during orientation estimates, CF was also compared to the reference system in the present study.

Series of long-distance walking (i.e., 15 minutes) on treadmill was performed at three different speeds (2.6 to 4.3 km/h) to validate the performance of all methods. Generally, the

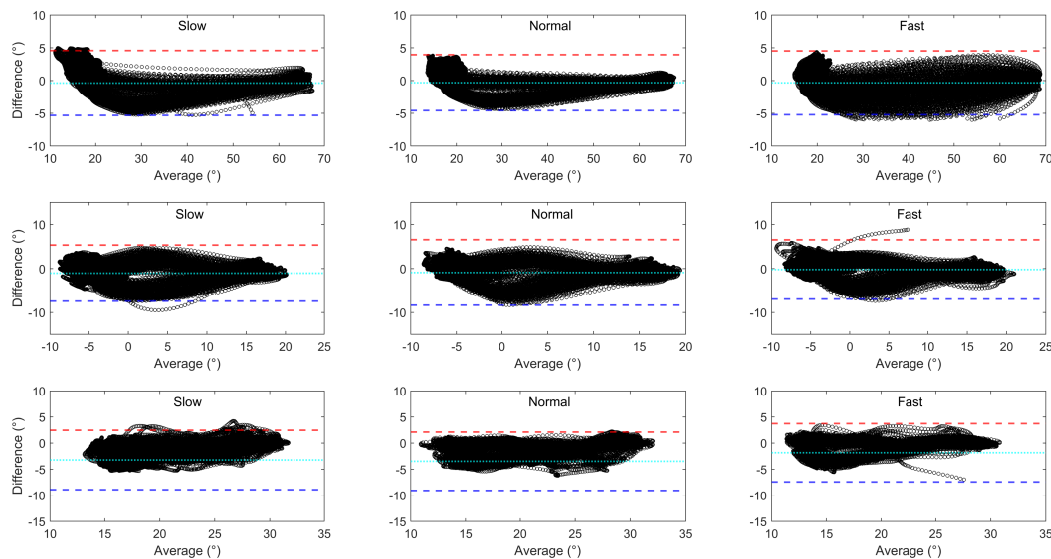


FIGURE 7. Bland and Altman plots of the difference between the NARX model and reference system in the sagittal (top panel), frontal (middle panel), and transverse plane (bottom panel) for slow, normal, and fast walking speed (2.6 to 4.3 km/h). The cyan dotted line corresponds to the mean, and the red and blue dashed lines represent the upper and lower limits of agreement (1.96 SD), respectively.

bias \pm precision values and RMSEs of NARX and PI in the sagittal plane are comparable with other studies estimating knee flexion-extension [1], [12], [15]. The correlation values between the two methods and the reference system are extremely high (between 0.97 and 0.99). With the lowest biases and RMSEs, results of current study showed that NARX is capable of providing consistent knee flexion-extension estimates for long-term walking at different speeds.

Similar to the sagittal plane, NARX provides consistent estimates of knee angle with a better accuracy and precision in the frontal plane. The results are further confirmed by the good agreement to the reference system.

For knee angle in the transverse plane, NARX is also consistent in joint angle computation with comparable bias values at three different walking speeds. PI exhibits relatively limited performance in the transverse plane, mainly due to the property of output de-personalization which produces symmetrical output trajectories along the horizontal axis. As shown in Fig. 6, PI estimation for knee angle in the transverse plane has a symmetrical feature along a line parallel to the horizontal axis. However, the physical knee internal-external rotation shows no line of symmetry parallel to the horizontal axis. The symmetrical property of PI was highlighted in Holgate *et al.* as a drawback, and the performance error was handled by tuning the control system to compensate this error. However, it is worth noting that the PI was used to provide feedback for the tibia flexion-extension where the error is minimal compared to the other rotations (i.e., sagittal and frontal plane) [51].

Good performance was observed for the comparisons between CF and the reference system in the sagittal and frontal

planes. As showed in Table 2 and 3, CF are presented with comparable biases and RMSEs for slow, normal, and fast level walking. Larger errors were produced with increasing walking speed in the sagittal plane due to higher translational and angular acceleration, where the translational acceleration affects sensor accuracy while the high frequency component of angular acceleration is blocked by the low pass filter. However, those errors are within the acceptable range. The observations suggest that CF is an appropriate approach for knee angle computation. High correlation values (between 0.94 and 0.99) recorded in the sagittal and frontal planes further validates the performance of CF in joint angle estimation. Results demonstrated by CF support the option of using sagittal plane orientation as the target output for training the proposed NARX model. As reflected in Table 2 - 4, the ability of NARX to accurately estimate 3D knee angle also suggested that the trained NARX was capable to replicate the performance of CF in estimating segmental orientation for all movement planes. Furthermore, Fig. 7 showed consistent average point-to-point biases for all subjects throughout the entire measurement time interval, suggesting stable performance of the proposed NARX in long-term knee angle estimation.

The dynamic behavior and rise time of knee angle trajectories are both method-dependent variables in this study, which explain the variation between methods at the beginning and end of the random 10 seconds windows illustrated in Fig. 6. Referring to Fig. 6, the NARX model demonstrated better ability to capture changes of higher frequency in the input signals. Whereas, PI and CF smoothed the input signals as the low-pass filter was included in both methods.

Well-known by its simplicity in data fusion, CF is recognized as one of the classic techniques that computes segmental orientation effectively, in which its capability is reflected in the results of current study. Despite its robustness, application of CF incorporating accelerometer and gyroscope, as demonstrated in the current study, is limited to measurements in 2-DoF, with measurement in the transverse plane negatively affected by the existence of gravitational acceleration. Sensory system featuring magnetometer is the most common alternative to such restriction. The local magnetic north provides a supplementary reference axis to the system, enabling 3D orientation measurement of body segments. Nevertheless, the existence of ferromagnetic interference greatly reduces the sensitivity of magnetometer. The issue remains a major challenge to the efficiency and reliability of such system, especially in clinical environment which comprises mainly of ferromagnetic materials and magnetic field-based devices [34]. In this context, the trained NARX has the advantage of computing 3D segmental orientation using only gyroscopes, avoiding the negative effects of accelerometer and magnetometer. Though trained using data in the sagittal plane, overall results of the present study demonstrated that the proposed NARX model is capable to produce low error estimates of knee angle in all movement planes, with good agreement to the reference system for different subjects and three ambulation speeds. Moreover, gait events detection for system reset, which might be difficult in high speed movements or not significant in pathological gait [53], is not required in the algorithm. This affirms the feasibility of NARX in real-time, varying speed applications, and clinical gait assessments.

Unlike most existing studies, validation of proposed algorithms involves the comparison between the IMU system attached to body segments and the reference optical system with reflective markers attached to body anatomical landmark, instead of attaching markers onto the sensor units. With both the IMUs and reflective markers attached directly to the skin, different degree of soft tissue artefacts arise from both systems were taken into account in this study. Lower limb segmental orientation was measured independently by both systems with their associating measurement errors, allowing actual accuracy assessment of the proposed systems with respect to the gold standard [54].

A limitation of the study is that all trials involved only able-bodied individuals. Movement disorders which lead to abnormal gait patterns might develop greater measurement error for inertial-based sensory system. In spite of that, results of the study show great potential of NARX to evaluating gait patterns of varying categories. Future work includes complete joint angle measurement for different locomotion activities in normal and pathological gaits. The 6-minute walk test (6MWT), for instance, being a popular clinical tool that evaluates a variety of physiological functionalities, is generally limited to the standardized outcome of 6MWT distance. Gait patterns and other kinematic parameters are frequently not considered in the test [55]. As such, it would be practicable to conduct gait evaluation such as the 6MWT

that measures body segment orientation or joint angles using the NARX which does not require dedicated space while providing comprehensive data to analyze specific functional status in the clinical environment.

V. CONCLUSION

The present study demonstrated that NARX neural network is feasible for ambulatory measurement of body segment orientation. Avoiding integration error, translational acceleration and ferromagnetic interference, NARX is capable to compute 3D knee angle with good agreement to the reference system. The proposed NARX model generally outperformed PI for slow, normal, and fast walking in all movement planes in terms of estimation error (Table 2 - 4). Although presented with higher measurement error, PI could be efficient in activity monitoring involving only pattern recognition. Both methods in this study provide simple and rapid processing of gyroscope signals, showing great potential for real-time and clinical applications.

ACKNOWLEDGMENT

The authors would like to express their gratitude to F. Dadashi, P. Morel, and J. Gramiger for their help and assistance with data collection, and all the subjects for their participation in this study.

REFERENCES

- [1] J. Favre, B. M. Jolles, R. Aissaoui, and K. Aminian, "Ambulatory measurement of 3D knee joint angle," *Journal of Biomechanics*, vol. 41, no. 5, pp. 1029–1035, 2008.
- [2] K. Liu, T. Liu, K. Shibata, Y. Inoue, and R. Zheng, "Novel approach to ambulatory assessment of human segmental orientation on a wearable sensor system," *Journal of Biomechanics*, vol. 42, no. 16, pp. 2747–2752, 2009.
- [3] J. Perry, *Gait analysis: Normal and pathological function*. New Jersey: SLACK Incorporated, 1992.
- [4] J. B. Saunders, V. T. Inman, and H. D. Eberhart, "The major determinants in normal and pathological gait," *Journal of Bone and Joint Surgery. American volume*, vol. 35, pp. 543–558, 1953.
- [5] M. R. Tucker, J. Olivier, A. Pagel, H. Bleuler, M. Bouri, O. Lambercy, J. R. Del Millán, R. Riener, H. Vallery, and R. Gassert, "Control strategies for active lower extremity prosthetics and orthotics: A review," *Journal of NeuroEngineering and Rehabilitation*, vol. 12, no. 1, pp. 1–30, 2015.
- [6] M. W. Whittle, "Clinical gait analysis: A review," *Human Movement Science*, vol. 15, no. 3, pp. 369–387, 1996.
- [7] R. Takeda, S. Tadano, M. Todoh, M. Morikawa, M. Nakayasu, and S. Yoshinari, "Gait analysis using gravitational acceleration measured by wearable sensors," *Journal of Biomechanics*, vol. 42, no. 3, pp. 223–233, 2009.
- [8] R. E. Mayoitia, A. V. Nene, and P. H. Veltink, "Accelerometer and rate gyroscope measurement of kinematics: An inexpensive alternative to optical motion analysis systems," *Journal of Biomechanics*, vol. 35, no. 4, pp. 537–542, 2002.
- [9] P. Picerno, A. Cereatti, and A. Cappozzo, "Joint kinematics estimate using wearable inertial and magnetic sensing modules," *Gait & Posture*, vol. 28, no. 4, pp. 588–595, 2008.
- [10] F. Alonge, E. Cucco, F. D'Ippolito, and A. Pulizzotto, "The use of accelerometers and gyroscopes to estimate hip and knee angles on gait analysis," *Sensors (Basel)*, vol. 14, no. 5, pp. 8430–8446, 2014.
- [11] W. Tao, T. Liu, R. Zheng, and H. Feng, "Gait analysis using wearable sensors," *Sensors (Basel)*, vol. 12, no. 2, pp. 2255–2283, 2012.
- [12] S. Šljajpah, R. Kamnik, and M. Munih, "Kinematics based sensory fusion for wearable motion assessment in human walking," *Computer Methods and Programs in Biomedicine*, vol. 116, no. 2, pp. 131–144, 2014.

- [13] K. Tong and M. H. Granat, "A practical gait analysis system using gyroscopes," *Medical Engineering & Physics*, vol. 21, no. 2, pp. 87–94, 1999.
- [14] T. Liu, Y. Inoue, and K. Shibata, "Development of a wearable sensor system for quantitative gait analysis," *Measurement*, vol. 42, no. 7, pp. 978–988, 2009.
- [15] S. Tadano, R. Takeda, and H. Miyagawa, "Three dimensional gait analysis using wearable acceleration and gyro sensors based on quaternion calculations," *Sensors (Basel)*, vol. 13, no. 7, pp. 9321–9343, 2013.
- [16] J. Morris, "Accelerometry—A technique for the measurement of human body movements," *Journal of Biomechanics*, vol. 6, no. 6, pp. 729–736, 1973.
- [17] R. Williamson and B. J. Andrews, "Detecting absolute human knee angle and angular velocity using accelerometers and rate gyroscopes," *Medical & Biological Engineering & Computing*, vol. 39, no. 3, pp. 294–302, 2001.
- [18] A. T. M. Willemsen, J. A. van Alsté, and H. B. Boom, "Real-time gait assessment utilizing a new way of accelerometry," *Journal of Biomechanics*, vol. 23, no. 8, pp. 859–863, 1990.
- [19] H. Dejnabadi, B. M. Jolles, and K. Aminian, "A new approach to accurate measurement of uniaxial joint angles based on a combination of accelerometers and gyroscopes," *IEEE Transactions on Biomedical Engineering*, vol. 52, no. 8, pp. 1478–1484, 2005.
- [20] H. Dejnabadi, B. M. Jolles, E. Casanova, P. Fua, and K. Aminian, "Estimation and visualization of sagittal kinematics of lower limbs orientation using body-fixed sensors," *IEEE Transactions on Biomedical Engineering*, vol. 53, no. 7, pp. 1385–1393, 2006.
- [21] R. Takeda, S. Tadano, A. Natorigawa, M. Todoh, and S. Yoshinari, "Gait posture estimation using wearable acceleration and gyro sensor," *Journal of Biomechanics*, vol. 42, no. 15, pp. 2486–2494, 2009.
- [22] M. D. Djurić-Jovičić, N. S. Jovičić, and D. B. Popović, "Kinematics of gait: New method for angle estimation based on accelerometers," *Sensors (Basel)*, vol. 11, no. 11, pp. 10571–10585, 2011.
- [23] B. Kemp, A. J. M. W. Janssen, and B. Van Der Kamp, "Body position can be monitored in 3D using miniature accelerometers and earth-magnetic field sensors," *Electroencephalography and Clinical Neurophysiology/Electromyography and Motor Control*, vol. 109, no. 6, pp. 484–488, 1998.
- [24] C. Bouten, K. Koekoek, M. Verduin, R. Kodde, and J. Janssen, "A triaxial accelerometer and portable data processing unit for the assessment of daily physical activity," *IEEE Transactions on Biomedical Engineering*, vol. 44, no. 3, pp. 136–147, 1997.
- [25] J. Favre, B. Jolles, O. Siegrist, and K. Aminian, "Quaternion-based fusion of gyroscopes and accelerometers to improve 3D angle measurement," *Electronics Letters*, vol. 42, no. 6, pp. 612–614, 2006.
- [26] H. J. Luinge and P. H. Veltink, "Measuring orientation of human body segments using miniature gyroscopes and accelerometers," *Medical and Biological Engineering and Computing*, vol. 43, no. 2, pp. 273–282, 2005.
- [27] H. Rehlinger and X. Hu, "Drift-free attitude estimation for accelerated rigid bodies," *Automatica*, vol. 40, no. 4, pp. 653–659, 2004.
- [28] H. J. Luinge and P. H. Veltink, "Inclination Measurement of Human Movement Using a 3-D Accelerometer with Autocalibration," *IEEE Transactions on Neural Systems and Rehabilitation Engineering*, vol. 12, no. 1, pp. 112–121, 2004.
- [29] P. H. Veltink, P. Slycke, J. Hemssems, R. Buschman, G. Bultstra, and H. Hermens, "Three dimensional inertial sensing of foot movements for automatic tuning of a two-channel implantable drop-foot stimulator," *Medical Engineering & Physics*, vol. 25, no. 1, pp. 21–28, 2003.
- [30] D. Roetenberg, H. J. Luinge, C. T. Baten, and P. H. Veltink, "Compensation of magnetic disturbances improves inertial and magnetic sensing of human body segment orientation," *IEEE Transactions on Neural Systems and Rehabilitation Engineering*, vol. 13, no. 3, pp. 395–405, 2005.
- [31] D. Roetenberg, P. J. Slycke, and P. H. Veltink, "Ambulatory position and orientation tracking fusing magnetic and inertial sensing," *IEEE Transactions on Biomedical Engineering*, vol. 54, no. 5, pp. 883–890, 2007.
- [32] K. J. O'Donovan, R. Kamnik, D. T. O'Keefe, and G. M. Lyons, "An inertial and magnetic sensor based technique for joint angle measurement," *Journal of Biomechanics*, vol. 40, no. 12, pp. 2604–2611, 2007.
- [33] Y. Tian, H. Wei, and J. Tan, "An adaptive-gain complementary filter for real-time human motion tracking with MARG sensors in free-living environments," *IEEE Transactions on Neural Systems and Rehabilitation Engineering*, vol. 21, no. 2, pp. 254–264, 2013.
- [34] P. Picerno, "25 years of lower limb joint kinematics by using inertial and magnetic sensors: A review of methodological approaches," *Gait and Posture*, vol. 51, pp. 239–246, 2017.
- [35] R. Mahony, T. Hamel, P. Morin, and E. Malis, "Nonlinear complementary filters on the special linear group," *International Journal of Control*, vol. 85, no. 10, pp. 1557–1573, 2012.
- [36] H. Fourati, "Heterogeneous data fusion algorithm for pedestrian navigation via foot-mounted inertial measurement unit and complementary filter," *IEEE Transactions on Instrumentation and Measurement*, vol. 64, no. 1, pp. 221–229, 2015.
- [37] B. J. West and N. Scafetta, "Nonlinear dynamical model of human gait," *Physical Review E*, vol. 67, no. 5, p. 051917, 2003.
- [38] D. J. Miller, N. Stergiou, and M. J. Kurz, "An improved surrogate method for detecting the presence of chaos in gait," *Journal of Biomechanics*, vol. 39, no. 15, pp. 2873–2876, 2006.
- [39] N. Scafetta, D. Marchi, and B. J. West, "Understanding the complexity of human gait dynamics," *Chaos: An Interdisciplinary Journal of Nonlinear Science*, vol. 19, no. 2, p. 026108, 2009.
- [40] A. Findlow, J. Y. Goulermas, C. Nester, D. Howard, and L. P. J. Kenney, "Predicting lower limb joint kinematics using wearable motion sensors," *Gait and Posture*, vol. 28, pp. 120–126, 2008.
- [41] A. J. Al-mahasneh, S. Anavatti, M. Garratt, and M. Pratama, "Applications of general regression neural networks in dynamic systems," in *Digital systems*, A. Vahid, Ed. Intechopen, 2018, pp. 133–154.
- [42] J. M. P. Menezes and G. A. Barreto, "Long-term time series prediction with the NARX network: An empirical evaluation," *Neurocomputing*, vol. 71, no. 16–18, pp. 3335–3343, 2008.
- [43] E. Diaconescu, "The use of NARX neural networks to predict chaotic time series," *WSEAS Transactions on Computer Research*, vol. 3, no. 3, pp. 182–191, 2008.
- [44] E. S. Grood and W. J. Suntay, "A joint coordinate system for the clinical description of three-dimensional motions: Application to the knee," *Journal of Biomechanical Engineering*, vol. 105, no. 2, pp. 136–144, 1983.
- [45] M. P. Kadaba, H. K. Ramakrishnan, and M. E. Wootten, "Measurement of lower extremity kinematics during level walking," *Journal of Orthopaedic Research*, vol. 8, no. 3, pp. 383–392, 1990.
- [46] P. Oliveira and A. Pascoal, "Navigation systems design: An application of multi-rate filtering theory," in *IEEE Oceanic Engineering Society. OCEANS'98*, Nice, France, 1998, pp. 1348–1353.
- [47] T. Lin, B. G. Horne, P. Tiño, and C. L. Giles, "Learning long-term dependencies in NARX recurrent neural networks," *IEEE Transactions on Neural Networks*, vol. 7, no. 6, pp. 1329–1338, 1996.
- [48] K. Levenberg, "A method for the solution of certain non-linear problems in least squares," *Quarterly of Applied Mathematics*, vol. 2, no. 2, pp. 164–168, 1944.
- [49] D. W. Marquardt, "An algorithm for least-squares estimation of nonlinear parameters," *SIAM Journal on Applied Mathematics*, vol. 11, no. 2, pp. 431–441, 1963.
- [50] A. I. Galushkin, *Neural networks theory*. Berlin: Springer-Verlag, 2007.
- [51] M. A. Holgate, T. G. Sugar, and A. W. Bohler, "A novel control algorithm for wearable robotics using phase plane invariants," in *2009 IEEE International Conference on Robotics and Automation*, Kobe, 2009, pp. 3845–3850.
- [52] J. M. Bland and D. G. Altman, "Statistical-methods for assessing agreement between 2 methods of clinical measurement," *The Lancet*, vol. 1, pp. 307–310, 1986.
- [53] D. Trojaniello, A. Cereatti, E. Pelosin, L. Avanzino, A. Mirelman, J. M. Hausdorff, and U. D. Croce, "Estimation of step-by-step spatio-temporal parameters of normal and impaired gait using shank-mounted magnetoinertial sensors: Application to elderly, hemiparetic, parkinsonian and choreic gait," *Journal of NeuroEngineering and Rehabilitation*, vol. 11, p. 152, 2014.
- [54] T. Seel, J. Raisch, and T. Schauer, "IMU-based joint angle measurement for gait analysis," *Sensors (Basel)*, vol. 14, no. 4, pp. 6891–6909, 2014.
- [55] F. A. Storm, A. Cesario, G. Reni, and E. Biffi, "Wearable inertial sensors to assess gait during the 6-minute walk test: A systematic review," *Sensors (Basel)*, vol. 20, no. 9, p. 2660, 2020.



and wearable technologies.

LAI KUAN THAM received B.Eng.Hons and M.Eng.Sc. in biomedical engineering from the University of Malaya, Malaysia. She is currently working towards the Ph.D. degree in biomedical engineering at the Centre for Applied Biomechanics (CAB), Department of Biomedical Engineering, Faculty of Engineering, University of Malaya. Her research interests include biomedical signal processing, biomechanics, motion capture, human movement monitoring and analysis, gait analysis,



KAMIAR AMINIAN received the M.S. degree in electrical engineering and the Ph.D. degree in biomedical engineering from the Ecole Polytechnique Fédérale de Lausanne (EPFL), Lausanne, Switzerland, in 1989. He is currently a Professor with the Institute of Bioengineering and the Director of the Laboratory of Movement Analysis and Measurement at EPFL. His research focuses on methodologies for human movement monitoring and analysis in real world conditions mainly based on wearable technologies, with an emphasis on gait, physical activity, and sport. His research aims to perform outcome evaluation in orthopaedics, to improve motor function and intervention programs in aging and patients with movement disorders and pain, and to identify metrics of performance in sport science. He is teaching in the areas of physiology and instrumentation, medical devices, biomechanics, and sports. He has authored or co-authored over 600 scientific papers published in reviewed journals, and presented at the international conferences and holds 12 patents related to medical devices.

...



NOOR AZUAN ABU OSMAN graduated from University of Bradford, UK with a B.Eng.Hons. in Mechanical Engineering, followed by MSc. and Ph.D. in Bioengineering from University of Strathclyde, UK. He is currently a practicing engineer and Professor of biomechanics with Faculty of Engineering, University of Malaya, Malaysia. His research interests are quite wide-ranging under the general umbrella of biomechanics. However, his main interests are the measurement of human movement, prosthetics design, the development of instrumentation for forces and joint motion, and the design of prosthetics, orthotics and orthopaedic. Prior to joining University of Malaya in 1996, he worked as mechanical and electrical engineer and actively involved in many consultancy projects, especially in the field of biomechanics and bio-mechanical engineering.



MOUAZ AL KOUZBARY received B.Sc. degree in mechatronics engineering from the University of Aleppo, Syria, and his M. Eng. Sc. degree in biomedical engineering from the University of Malaya, Malaysia. He is currently a Ph.D. candidate and research assistance at the Centre for Applied Biomechanics (CAB), Department of Biomedical Engineering, Faculty of Engineering, University of Malaya. His research interests include Artificial Intelligent control systems, machine learning algorithms, genetic algorithm, robotics, biomechanics, powered lower limb prostheses, and bio-inspired leg designs.